The American Journal of Pathology, Vol. 193, No. 5, May 2023

The American Journal of
PATHOLOGY
ajp.amjpathol.org

VASCULAR BIOLOGY, ATHEROSCLEROSIS, AND ENDOTHELIUM BIOLOGY

Genetic Deletion of FXR1 Reduces Intimal Hyperplasia and Induces Senescence in Vascular Smooth Muscle Cells

Cali B. Corbett,* Amanda St. Paul,* Tani Leigh,* Sheri E. Kelemen,* Amanda M. Peluzzo,* Rachael N. Okune,* Satoru Eguchi,† Dale S. Haines,‡ and Michael V. Autieri*

From the Department of Cardiovascular Sciences, Lemole Center for Integrated Lymphatics Research, the Cardiovascular Research Center,† and the Department of Medical Genetics and Molecular Biochemistry,‡ Lewis Katz School of Medicine at Temple University, Philadelphia, Pennsylvania*

Accepted for publication January 12, 2023.

Address correspondence to Michael V. Autieri, Ph.D., Department of Cardiovascular Sciences, Temple University School of Medicine, Room 1050, MERB 3500, N. Broad St., Philadelphia, PA 19140. E-mail: mautieri@temple.edu.

Vascular smooth muscle cells (VSMC) play a critical role in the development and pathogenesis of intimal hyperplasia indicative of restenosis and other vascular diseases. Fragile-X related protein-1 (FXR1) is a muscle-enhanced RNA binding protein whose expression is increased in injured arteries. Previous studies suggest that FXR1 negatively regulates inflammation, but its causality in vascular disease is unknown. In the current study, RNA-sequencing of FXR1-depleted VSMC identified many transcripts with decreased abundance, most of which were associated with proliferation and cell division. mRNA abundance and stability of a number of these transcripts were decreased in FXR1-depleted hVSMC, as was proliferation ($P < 0.05$); however, increases in beta-galactosidase ($P < 0.05$) and γH2AX ($P < 0.01$), indicative of senescence, were noted. Further analysis showed increased abundance of senescence-associated genes with FXR1 depletion. A novel SMC-specific conditional knockout mouse ($FXR1^{SMC/SMC}$) was developed for further analysis. In a carotid artery ligation model of intimal hyperplasia, $FXR1^{SMC/SMC}$ mice had significantly reduced neointima formation ($P < 0.001$) after ligation, as well as increases in senescence drivers p16, p21, and p53 compared with several controls. These results suggest that in addition to destabilization of inflammatory transcripts, FXR1 stabilized cell cycle–related genes in VSMC, and absence of FXR1 led to induction of a senescent phenotype, supporting the hypothesis that FXR1 may mediate vascular disease by regulating stability of proliferative mRNA in VSMC. *(Am J Pathol 2023, 193: 638–653; https://doi.org/10.1016/j.ajpath.2023.01.006)*

Vascular disease continues to account for over half of all mortality in the United States, Europe, and the developing world. It is a considerable medical and socioeconomic problem contributing to mortality associated with many conditions including myocardial infarction, stroke, renal failure, and peripheral vascular disease. Vascular smooth muscle cell (VSMC) activation plays a crucial role in the development of multiple vascular diseases, including atherosclerosis, restenosis, hypertension, and abdominal aortic aneurysm.[1–3] In response to proinflammatory and immune modulators, VSMC migrate into the vessel intima, synthesize cytokines and matrix proteins, and proliferate; this often leads to loss of lumen and tissue ischemia. Inflammation and proliferation are fundamental processes to the alteration of a homeostatic state or stress in every cell type involved in vascular disease. The inducible inflammatory response is complex and tightly regulated, requiring the coordination of signal-specific programs to regulate hundreds of genes. Complementary to transcription, post-transcriptional mechanisms are critical in regulating the balance of inflammation as the instability of inflammatory

Supported by NIH National Heart, Lung, and Blood Institute grants HL141108 and HL117724 (M.V.A.).

Disclosures: None declared.

Presented in abstract form at the American Heart Association Scientific Sessions, Philadelphia, PA (November 16–18, 2019) and ATVB Vascular Discovery, Seattle, WA (May 12–14, 2022).

Copyright © 2023 American Society for Investigative Pathology. Published by Elsevier Inc. All rights reserved.
https://doi.org/10.1016/j.ajpath.2023.01.006

and cell cycle mediator mRNAs permits a fine-tuned response to inflammatory and proliferative stimuli.[4,5] Regulation of mRNA stability allows the cell to rapidly modify gene expression, as needed, during disruptions to homeostasis.[6] Transcripts targeted for rapid degradation encode key regulatory proteins involved in cell growth, inflammation, and other responses to external stimuli.[7,8] RNA stability is regulated by a number of RNA-binding proteins (RBPs), which recognize *cis*-acting adenine and uridine-rich (AU-rich) elements (AREs) in the 3′ untranslated regions (UTR) of most of these labile mRNA transcripts.[5,9] RBPs can destabilize or stabilize mRNA transcripts, allowing for decreased or increased mRNA translation and protein synthesis, respectively. Tightly coordinated gene expression and mRNA stability are particularly relevant for the progression of many vascular diseases, which are often inflammatory and proliferative in nature. This mechanism is particularly applicable to VSMC, which make up the vast majority of cells in normal and inflamed arteries. In this regard, it is logical that RBPs that respond to inflammatory stimuli in VSMC may be key in the regulation of gene expression and, therefore, the vascular response to injurious stimuli. Nevertheless, the expression and participation of RBPs in vascular disease is an understudied, yet key, mechanism in disease progression.

The fragile X family of proteins includes fragile-X mental retardation protein (FMRP) as well as homologs fragile-X related proteins 1 and 2 (FXR1-1 and -2). FMRP is an RBP expressed primarily in neuronal tissues and is the most studied family member, as fragile X syndrome is caused by a transcriptional shutdown of this gene.[10] One FMRP family member, FXR1, is the only fragile X protein family member whose expression is significantly expressed in muscle cells, particularly heart, smooth, and skeletal muscle.[11–13] Global knockout of FXR1 in a mouse is lethal, with a striated muscle phenotype, and FXR1 has been described as the "muscle-homologue," analogous to the better-characterized FMR protein in neurons, suggesting a specialized role for this family member in muscle cell physiology.[13] FXR1 expression is increased in VSMC in atherosclerosis and restenosis, and in cultured primary human VSMC (hVSMC) response to oxidized low-density lipoprotein.[14] FXR1 is a putative mRNA destability protein, and plays a role in regulation of mRNA abundance in VSMC by binding to inflammatory mRNA. FXR1 may compete with mRNA stability protein HuR for occupancy on the 3′UTR of select transcripts, resulting in decreased mRNA stability. FXR1 is basally expressed in healthy arteries, but its expression is up-regulated in neointimal VSMC in a murine model of vascular restenosis and plaque VSMC in human atherosclerotic arteries.[14] Despite this, the causality of FXR1 expression in the vascular response to injury in a relevant animal model of vascular disease has not been reported.

In the current study, primary hVSMCs were used to identify transcripts regulated by FXR1 silencing by RNA sequencing. Depletion of FXR1 reduced the stability of a number of cell division–related transcripts, indicating that FXR1 stabilizes these transcripts. Proliferation and senescence were also dysregulated in these cells, indicating that at least in VSMC, FXR1 may act to stabilize as well as destabilize select mRNA transcripts, resulting in an unanticipated senescent phenotype.

In light of this finding, knockout mice with FXR1 conditionally deleted from smooth muscle cells (SMC) were generated and subjected to carotid artery ligation, a commonly used model of arterial injury. These mice were protected from neointimal hyperplasia, likely due to the decrease in proliferation and induction of senescence in VSMC lacking the FXR1 gene.

Materials and Methods

Generation of *FXR1*$^{SMC/SMC}$ Mice

FXR1$^{flox/flox}$ mice on the C57Bl/6 background were obtained from the FMR research resource at Baylor University and described in Mientjes et al.[13] Total knockout of the gene is lethal shortly after birth. Female FXR1$^{flox/flox}$ mice were crossed with congenic male C57BL/6 Myh11-CreERT2 mice as described in Wirth et al[15] because the allele is carried only on the Y chromosome, and appropriate offspring were identified by PCR-based genotyping. Because Myh11-CreERT2 resides on the Y chromosome, only male mice were used for these studies. Cre-Lox–mediated knockout of FXR1 was induced in 6-week–old male mice after intraperitoneal injection of 1 mg of tamoxifen (T-5648; Sigma-Aldrich, St. Louis, MO) per mouse per day for 5 consecutive days. Tamoxifen-mediated Cre recombinase expression is one of the most widely used tools for gene modification.[16] Briefly, the male *FXR1*$^{SMC/SMC}$ mice have loxP sites flanking the FXR1 gene and carry a smooth muscle–specific Cre recombinase coupled to a mutated estrogen receptor on the Y chromosome. Under physiological conditions, this mutated estrogen receptor does not bind its ligand, but when the mouse is injected intraperitoneally with tamoxifen (a synthetic hormone), the receptor is activated, and cre translocates from the nucleus to interact with the loxP sites and cleave out the FXR1 gene in SMC.[17] SMC-specific excision of FXR1 was validated by Western blot and immunohistochemistry. No gross differences between FXR1 knockout and wild-type mice were observed in any offspring.

Carotid Artery Ligation

Age-matched male mice (ages 8 to 12 weeks) were used for these studies. The ligation model of injury was performed as described previously.[18] Briefly, mice were anesthetized by inhalation of isoflurane (induction 3% to 5%, maintenance 1% to 2%). The left common carotid artery was dissected and ligated near the bifurcation. After 28 days, mice were

euthanized, and tissue was prepared for immunohistochemistry and morphological analysis. All animal procedures followed Temple University Institutional Animal Care and Use Committee–approved protocols.

VSMC Culture, Proliferation Assays

Primary human coronary artery VSMC were obtained as cryopreserved secondary culture from LifeLine, Inc. (Oceanside, CA), and maintained as previously described.[14,19,20] VSMC were used from passages 2 to 4. For mouse VSMC (mVSMC), abdominal aorta from control and *FXR1*$^{SMC/SMC}$ mice were excised, endothelial layer removed, and VSMC isolated as described.[18,21] VSMC were cultured in Dulbecco's modified Eagle's medium supplemented with 20% fetal calf serum. Greater than 95% of isolated cells were SMC actin positive from initial passage. Two different proliferative assays were performed. Proliferation was assayed by the BrdU (bromodeoxyuridine) kit from Cell Signaling Technology, Inc. (Danvers, MA), according to the manufacturer's instructions. Flow cytometry was performed as previously described.[22] Briefly, cells were transfected with FXR1 siRNA or a scrambled control and cultured for 3 days before they were trypsinized, fixed in ice-cold 70% ethanol, and stained with propidium iodide (PI) using the FxCycle PI/RNase staining solution from Invitrogen (Waltham, MA; cat#2110506) according to the manufacturer's instructions. Samples were analyzed on a BD LSR II flow cytometer (BD Biosciences, San Jose, CA).

β-gal and γH2AX Staining

hVSMC were transfected with FXR1 siRNA or a scrambled control and seeded into chamber slides. Seventy-two hours after transfection, cells were fixed and stained for common senescence markers γH2AX (Novus, Littleton, CO; cat# NB100-384) and β-galactosidase (β-gal) using a kit from Cell Signaling Technology, Inc. (cat# 6813S) according to the manufacturer's instructions. VSMC were also isolated from *FXR1*$^{SMC/SMC}$ mice, seeded into chamber slides, transduced with 100 multiplicity of infection of GFP or Cre adenovirus, and stained for β-gal after 72 hours using the kit referenced above.

Immunohistochemistry and Quantitative Morphology

Digitized images of hematoxylin and eosin–stained carotid artery cross sections were measured and averaged from at least three representative 5-μm–thick stained tissue sections at least 75 to 100 μm apart per carotid artery using Image-Pro Plus software version 4.0 (Media Cybernetics, Rockville, MD) as previously described.[20,21,23] At least six mice per group were used for morphology and immunohistochemistry. The circumference of the lumen, the area encircled internal elastic lamina, and the external elastic lamina were quantitated. The medial area was calculated by subtracting the area defined by the internal elastic lamina from the area defined by the external elastic lamina, and intimal area calculated as the difference between the area inside the internal elastic lamina and the luminal area. Tissue fixation, processing, and immunohistochemical staining was performed as described.[21,24,25]

Transfection, RNA Extraction, and Quantitative RT-PCR

FXR1 depletion in primary hVSMC was performed using 10 nmol/L ON-TARGET plus SMARTpool FXR1 siRNA containing a mixture of four siRNAs that target human FXR1, purchased from Dharmacon (Lafayette, CO). Cells were transfected using an Amaxa Nucleofector 2b device from Lonza (Walkersville, MD) as described previously.[26] RNA from cultured VSMC was isolated and reverse transcribed into cDNA, as previously described, and target genes were amplified using an Applied Biosystems StepOnePlus Real-Time PCR System[19,21,26] (Applied Biosystems, Waltham, MA) and described in detail in Table 1. Multiple mRNAs (Ct values) were quantitated simultaneously by the PCR machine software. Primer pairs were purchased from Integrated DNA Technologies (Coralville, IA), and SYBR green was used for detection. For RNA stability, cells were stimulated for 16 hours with tumor necrosis factor α (TNFα; 10 ng/nL) and then treated with 10 ng/mL actinomycin D as previously described,[14,26] and RNA was extracted at various times after actinomycin D addition (0, 2, 4 hours).

Adenoviral Knockout of FXR1

Primary abdominal aortic VSMC were isolated from *FXR1*$^{SMC/SMC}$ mice as described previously[16,19] and cultured in Dulbecco's modified Eagle's medium supplemented with 20% fetal calf serum. Cells were transduced with 100 multiplicity of infection of a control GFP adenovirus or 100 multiplicity of infection of a Cre adenovirus to knock out FXR1. Subsequent procedures were performed following 72 hours of transduction to ensure knockout of the gene.

RNA Sequencing

Library preparation and unbiased RNA sequencing was performed by GENEWIZ (South Plainfield, NJ). Total RNA was isolated from primary hVSMC transfected with FXR1 siRNA (5 nmol/L) or scrambled control, serum starved or stimulated with 10 ng/mL TNFα for 6 hours; libraries were sequenced using a 1× 100-bp single-end rapid run on the HiSeq2500 platform, and a comparison of gene expression using DESeq2. The Wald test was used to generate P values and log2 fold changes. Genes with a P value <0.05 and absolute log2 fold change >1 were called as differentially expressed genes. Significantly differentially expressed genes were clustered by their gene ontology, and the

Table 1 Human and Mouse Primer Sets Used for Quantitative PCR Analysis

Gene	Forward primer sequence	Reverse primer sequence
Human		
GAPDH	5′-CGAGAGTCAGCCGCATCTT-3′	5′-CCCCATGGTGTCTGAGCG-3′
FXR1	5′-GAGTTACCGCCATTGAGCTAG-3′	5′-ACTTTTCCAACGAGATTCCTAGG-3′
TNFA	5′-GGTCTACTTTGGGATCATTGC-3′	5′-GAAGAGGTTGAGGGTGTCTG-3′
CDK1	5′-ACAAAGGAACAATTAAACTGGCTG-3′	5′-CTGGAGTTGAGTAACGAGCTG-3′
LIN9	5′-GACTGAACAAGGACCTAAACAAAG-3′	5′-CATGCCGAACAATTTCCTGTG-3′
BUB1	5′-CCGAGTCTCAGAAAATACCAGG-3′	5′-AAATGGAGAAAGGTACACTGGG-3′
GJA5	5′-GTTTTGGCATCTGTTCCCTG-3′	5′-CGGAATATGAAGAGGACAGTGAG-3′
CD93	5′-CAGACAGTTACTCCTGGGTTC-3′	5′-GTGGCTGGTGACTCTAGTG-3′
MKI67	5′-GACCCAGCACTCCAAAGAAA-3′	5′-TCTGCGCTCTACCTACTACAA-3′
CDKN3	5′-GCCAGCTGCTGTGAAATAATG-3′	5′-GTAGGAGACAAGCAGCTACAAG-3′
HMGB1	5′-GAATCTCTATGTTGCCCAGGT T-3′	5′-CAGTGGTGTGTCCCTGTAATC-3′
IL8	5′-CCAGGAAGAAACCACCGGA-3′	5′-GAAATCAGGAAGGCTGCCAAG-3′
IL1A	5′-CTGAAGGAGATGCCTGAGATAC-3′	5′-GATGGGCAACTGATGTGAAATAG-3′
IL6	5′-CCAGGAGAAGATTCCAAAGATGTA-3′	5′-CGTCGAGGATGTACCGAATTT-3′
IL1B	5′-TCCCCAGCCCTTTTGTTGA-3′	5′-TTAGAACCAAATGTGGCCGTG-3′
MMP9	5′-GAACTTTGACAGCGACAAGAAG-3′	5′-CGGCACTGAGGAATGATCTAA-3′
CXCL11	5′-GTGTGAAGGGCATGGCTATAG-3′	5′-CACTTTCACTGCTTTTACCCC-3′
HMGB2	5′-GAAGTGTTCGGAGAGATGGAAG-3′	5′-CACCTTTGGGAGGAACGTAAT-3′
MCP1	5′-AGCAGAAGTGGGTTCAGGATT-3′	5′-TGTGGAGTGAGTGTTCAAGTCT-3′
Mouse		
Gapdh	5′-GGAGAAACCTGCCAAGTATGA-3′	5′-TCCTCAGTGTAGCCCAAGA-3′
Fxr1	5′-GAACGCATGGCACTAACATAC-3′	5′-CACAAATTCCAAGAAACCTCTAGC-3′
Cdk1	5′-TTGAAGAGGCAACCGAGTAAG-3′	5′-GGCGTTAGGTCATCCATCAA-3′
Cdkn3	5′-GACTTGGAAGATCCTGTCTTGT-3′	5′-GACATCTCGAAGGCTGTCTATG-3′
Bub1	5′-CCCTGGAGTAGGAAGCTAGT-3′	5′-ATGGTGGTCTCACAACAAGAA-3′
Mki67	5′-GACCCAGCACTCCAAAGAAA-3′	5′-TCTGCGCTCTACCTACTACAA-3′
Cdkn2a (*p16*)	5′-GTGTGCATGACGTGCGGG-3′	5′-GCAGTTCGAATCTGCACCGTAG-3′
Cdkn1a (*p21*)	5′-AACATCTCAGGGCCGAAA-3′	5′-TGCGCTTGGAGTGATAGAAA-3′
Trp53 (*p53*)	5′-GTATTTCACCCTCAAGATCC-3′	5′-TGGGCATCCTTTAACTCTA-3′
Hmgb1	5′-CCCTACTAAAGAAGACCTGAGAATG-3′	5′-AGCCAGCGTTCTTGTGATAG-3′

enrichment of gene ontology terms was tested using the Fisher exact test (GeneSCF v1.1-p2; *https://github.com/genescf*). Log2(Group 2 mean normalized counts/Group 1 mean normalized counts) = log2FoldChange.

RNA Immunoprecipitation

For RNA immunoprecipitation (RIP), hVSMC were transduced with AdenoFXR1 prior to serum starvation for 48 hours. Cells were treated with TNFα for 24 hours and lysed in IP buffer with RNase inhibitor. Samples were divided and half were incubated with IgG control beads or Flag-conjugated beads for 4 hours at 25°C. The beads were then centrifuged and washed 5× in IP buffer. Trizol was added to the pelleted beads, and RNA was extracted and reverse transcribed to cDNA. Pellets were sent for unbiased RNA sequencing as described above, or for quantitative RT-PCR for the transcripts indicated.

Western Blotting and Protein Determination

hVSMC and mVSMC extracts were prepared as described.[20,21,24] Membranes were incubated with a 1:2000 to 9000 dilution of primary antibody, and a 1:2000 dilution of secondary antibody. Glyceraldehyde 3-phosphate dehydrogenase (GAPDH) and FXR1 were from Cell Signaling Technology (cat# 2118S and 2295S, respectively), HSC70 and p53 from Santa Cruz Biotechnology (Dallas, TX; cat# sc-7298 and sc-126), BUB1 and CDKN31 from Abcam, Inc. (Cambridge, UK; cat# ab195268 and ab175393, respectively), and CDK1 from Boster, Inc. (Pleasanton, CA; cat# PB9533). Secondary antibodies were from Cell Signaling Technology (anti-rabbit IgG cat#7074S, anti-mouse IgG cat# 7076S). Reactive proteins were visualized using enhanced chemiluminescence (Amersham, Piscataway, NJ) according to the manufacturer's instructions. Relative intensity of bands were normalized to GAPDH or HSC70, and quantitated by scanning image analysis and the ImageJ densitometry program software version 1.53a (NIH, Bethesda, MD; *https://imagej.net/ij/index.html*).

Statistics

Results are expressed as mean ± SEM. Differences between groups were evaluated with the use of analysis of variance to evaluate differences between individual mean values or by *t*-tests where appropriate.

Results

Depletion of FXR1 Modifies Abundance of Proliferation-Associated Transcripts

FXR1 is an mRNA binding protein and presumed to be an mRNA destability factor. Therefore, the initial goal of the study was to identify inflammation-responsive genes whose abundance might be modified by deletion of FXR1. First, FXR1 expression in cultured primary hVSMC was shown to be responsive to inflammatory stimuli. Figure 1, A–C, shows that FXR1 mRNA and protein abundance in VSMC are increased in response to TNFα stimulation. Because TNFα is a potent proinflammatory cytokine and a major driver of vascular inflammation, and TNFα induces FXR1 mRNA and protein expression, the study aimed to identify genes whose mRNA abundance would be altered by FXR1 knockdown in primary hVSMC in the presence or absence of TNFα. Figure 1D shows the effectiveness of FXR1 siRNA transfection in knock down of the FXR1 protein. Figure 1, E and F, shows volcano plots of genes whose expression was significantly altered ($P \leq 0.05$) by

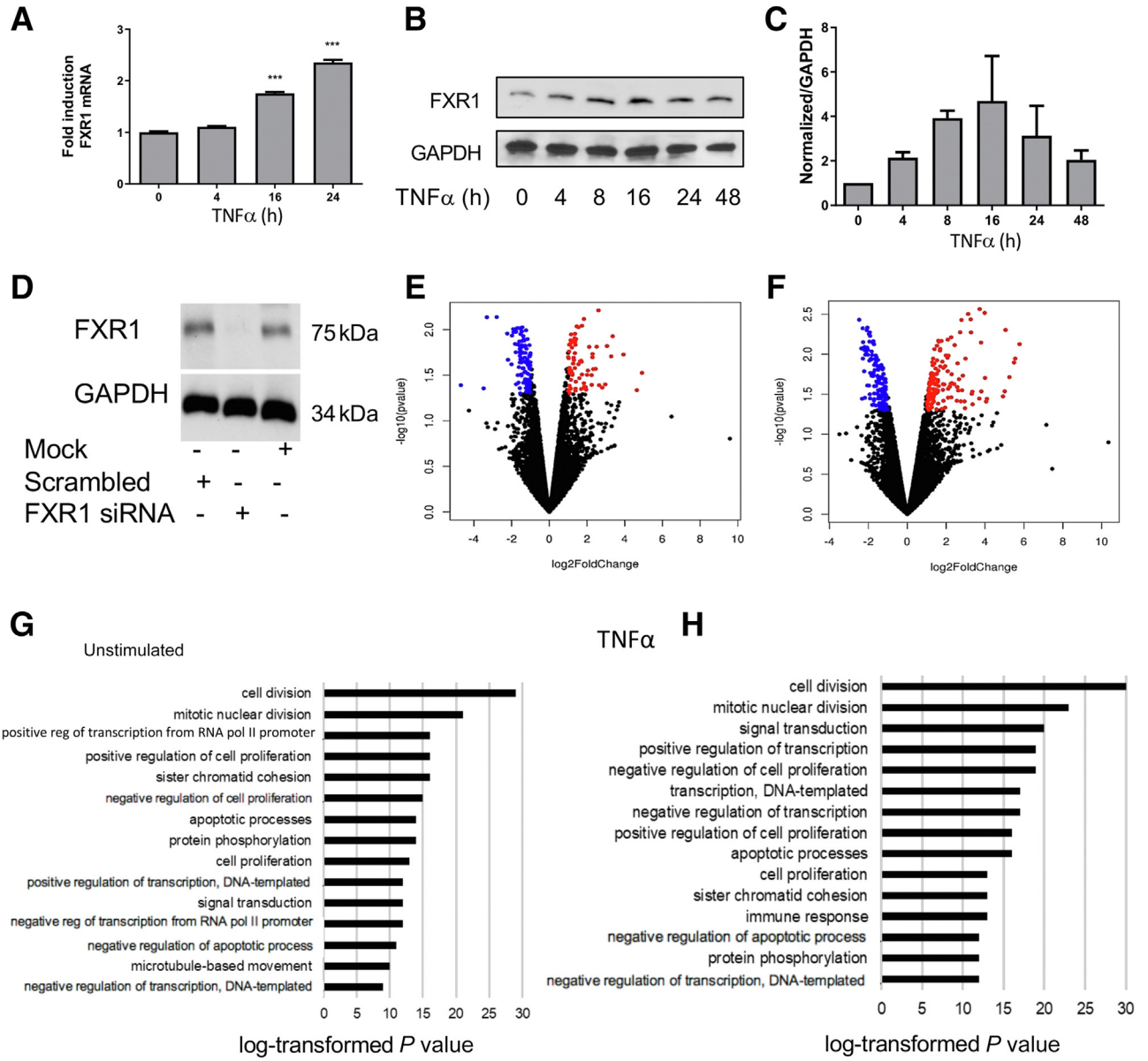

Figure 1 Expression and FXR1-dependent gene expression in stimulated human vascular smooth muscle cells (hVSMC). **A:** FXR1 mRNA expression is induced by TNFα stimulation in hVSMC. **B** and **C:** FXR1 protein expression is induced by TNFα stimulation. **D:** FXR1 SMARTpool siRNA effectively knocks down FXR1 protein in hVSMC 72 hours after transfection. **E**–**G:** Volcano plots comparing mRNA abundance detected from RNA sequencing of FXR1 siRNA and control siRNA transfected hVSMC serum-starved 48 hours (**E**), and stimulated with TNFα for 6 hours (**F**). Significantly down-regulated and up-regulated transcripts are represented by blue and red data points, respectively. Gene ontology analysis of RNAseq in unstimulated (**G**), and TNFα-stimulated hVSMC. **H:** Enhanced expression of transcripts associated with cell division. $***P < 0.001$.

the loss of FXR1 in starved and TNFα-stimulated VSMC, respectively. It is apparent from these plots that in both serum-starved and TNFα-stimulated VSMC, the loss of FXR1 resulted in more transcripts with increased abundance compared with those with reduced abundance, which is consistent with an mRNA destability protein.

Figure 1, G and H, shows Gene Ontology profiles from both unstimulated and TNFα-stimulated VSMC. Categories were enriched for genes that participate in cell division, mitosis, proliferation, and as expected, mRNA metabolism. Considering that FXR1 is an mRNA binding protein and a putative mRNA destability factor, it was surprising that there were a number of genes whose abundance were decreased by FXR1 knockdown, suggesting that FXR1 participated in stabilization of those transcripts. It was particularly interesting that in FXR1-depleted VSMC, over 90% of these transcripts were associated with cell division and proliferation (Table 2). This suggested a function for FXR1 in regulation of VSMC proliferation, perhaps by stabilization of transcripts important in cell division.

Expression of a number of these proliferation-associated transcripts was validated by quantitative RT-PCR in response to TNFα stimulation (Figure 2A). Because FXR1 is generally considered to be an RBP with effects on mRNA stability, the mRNA stability of transcripts modified by FXR1 abundance using the RNA polymerase inhibitor actinomycin D was determined next. Figure 2B shows that the mRNA stability of CDK1, BUB1, MKI67, and CDKN3, all genes associated with cell division, is significantly decreased with FXR1 knock down. The decrease in mRNA abundance was reflected in reduced protein abundance by Western blot. Figure 2C shows that the protein abundance of these genes is significantly decreased in TNFα-stimulated hVSMC when FXR1 is knocked down.

Table 2 Genes Reduced between the Maximal Amount and 1.75-Fold Whose Abundance Were Decreased by FXR1 Knockdown

Gene ID	Gene name	log2FoldChange	*P* value
ENSG00000169607	*CKAP2L*	−1.81	0.18
ENSG00000274290	*HIST1H2BE*	−1.83	0.01
ENSG00000024526	*DEPDC1*	−1.83	0.009
ENSG00000142945	*KIF2C*	−1.85	0.011
ENSG00000072571	*HMMR*	−1.87	0.01
ENSG00000123485	*HJURP*	−1.9	0.02
ENSG00000100526	*CDKN3*	−1.91	0.04
ENSG00000164109	*MAD2L1*	−1.92	0.01
ENSG00000138160	*KIF11*	−1.93	0.01
ENSG00000129195	*PIMREG*	−1.93	0.03
ENSG00000170312	*CDK1*	−1.94	0.01
ENSG00000137812	*KNL1*	−1.95	0.01
ENSG00000066279	*ASPM*	−1.97	0.01
ENSG00000276903	*HIST1H2AL*	−1.97	0.02
ENSG00000124575	*HIST1H1D*	−2.02	0.01
ENSG00000274641	*HIST1H2BO*	−2.03	0.01
ENSG00000278272	*HIST1H3C*	−2.05	0.01
ENSG00000197153	*HIST1H3J*	−2.05	0.02
ENSG00000276410	*HIST1H2BB*	−2.07	0.01
ENSG00000138778	*CENPE*	−2.08	0.01
ENSG00000183598	*HIST2H3D*	−2.1	0.01
ENSG00000080986	*NDC80*	−2.11	0.01
ENSG00000125810	*CD93*	−2.15	0.01
ENSG00000183814	*LIN9*	−2.18	0.04
ENSG00000073849	*ST6GAL1*	−2.19	0.01
ENSG00000117399	*CDC20*	−2.2	0.01
ENSG00000175063	*UBE2C*	−2.22	0.02
ENSG00000169679	*BUB1*	−2.27	0.01
ENSG00000163535	*SGO2*	−2.28	0.01
ENSG00000112984	*KIF20A*	−2.29	0
ENSG00000158402	*CDC25C*	−2.32	0.04
ENSG00000148773	*MKI67*	−2.36	0.01
ENSG00000112742	*TTK*	−2.47	0

Genes found on NCBI Gene database at *https://www.ncbi.nlm.nih.gov/gene*.

FXR1 Interacts with Proliferation-Associated mRNA Transcripts

Many labile mRNAs are regulated at the post-transcriptional level by AU-rich elements (AREs) in the 3′UTR.[27,28] The ARE provides a binding site for trans-acting RBPs, and it has been previously shown that FXR1 interacts with AREs.[14] One commonality shared by BUB1, CDK1, CDKN3, and MKI67 is the presence of AREs in the 3′UTR or intronic regions of their mRNA (Figure 3A), which may provide an explanation as well as potential mechanism for FXR1 interaction with these transcripts.[29,30] With this in mind, RNA immunoprecipitation sequencing (RIPseq) was performed to identify mRNAs that might specifically interact with FXR1. For these experiments, FLAG-tagged FXR1 was transduced into hVSMC that were serum starved, then stimulated with TNFα. Gene Ontology analysis of transcripts that immunoprecipitated with FXR1 after TNFα-stimulation, compared with unstimulated VSMC, revealed an informative view of FXR1 mRNA transcript interactions in response to TNFα. Gene Ontology analysis demonstrated enhancement of transcripts associated with regulation of cell proliferation, transcription from RNA, and inflammatory responses (Figure 3B). Importantly, mRNA for BUB1, CDK1, MIK67, and CDKN3 all contain AREs in their 3′UTR and were all identified as pulled down with FXR1. FXR1's interactions with these mRNAs were validated by an independent standard RIP RT-PCR (Figure 3C), indicating that FXR1 interacted with these mRNA transcripts.

Depletion of FXR1 Induces Senescence and Senescence-Associated Secretory Phenotype Expression in VSMC

Because FXR1 expression modified the mRNA stability and protein abundance of several critical cell cycle and proliferation-associated proteins, experiments were performed to test the hypothesis that FXR1 depletion would

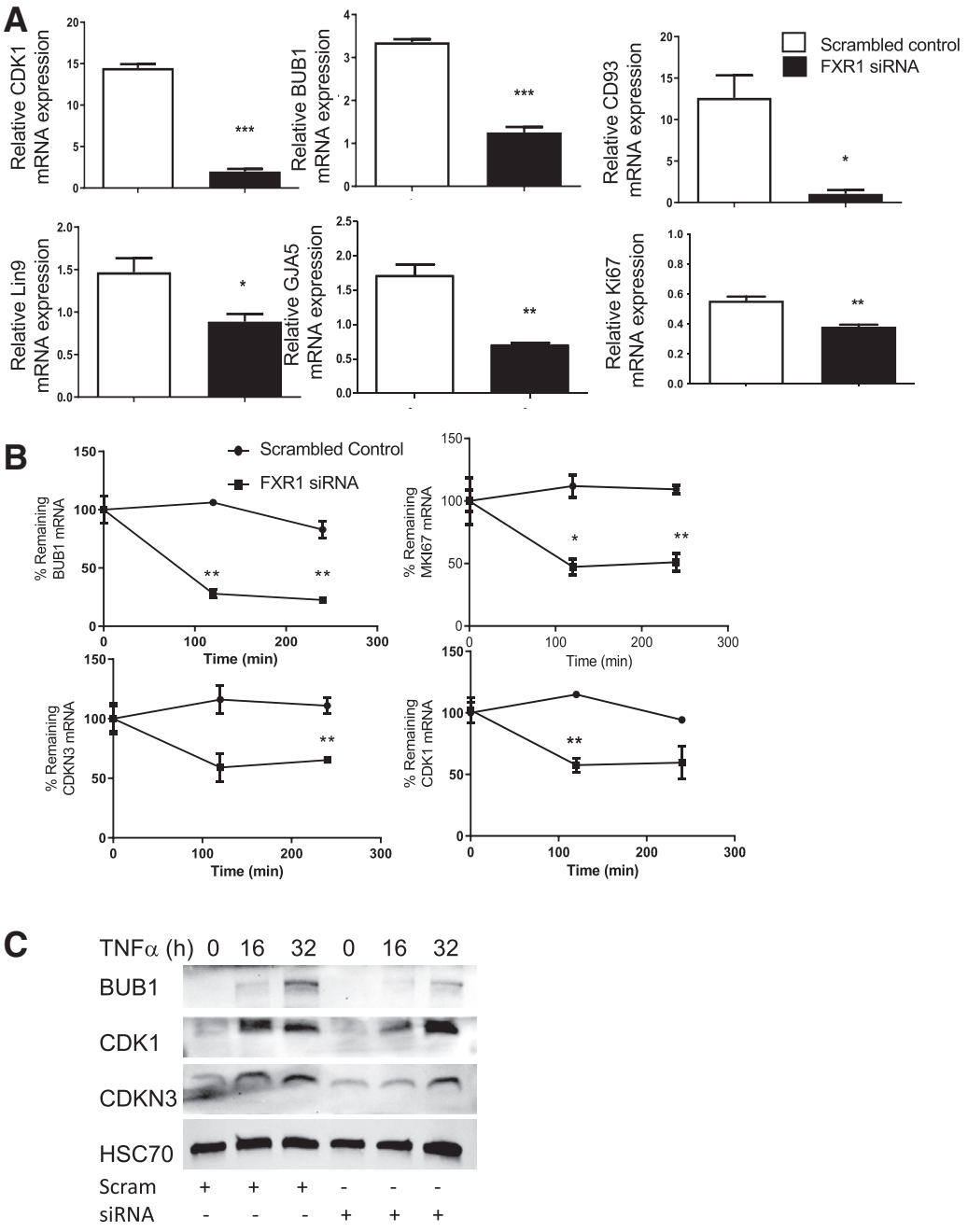

Figure 2 FXR1 deletion results in decreased cell cycle gene expression and mRNA stability. **A:** Quantitative RT-PCR of mRNA abundance of cell division–associated genes in TNFα-stimulated human vascular smooth muscle cells (hVSMC) transfected with scrambled control or FXR1-specific siRNA. **B:** Deletion of FXR1 decreases mRNA stability of cell division–associated genes. RNA was isolated from hVSMC stimulated with TNFα, then treated with actinomycin D. RNA was quantitated at the indicated times after addition of actinomycin D. **C:** Representative Western blot of cell division–associated genes in TNFα-stimulated hVSMC. Protein was extracted at the indicated times after stimulation and immunoblotted with the indicated antibodies. $n \geq 3$ experiments (**A** and **B**). $^{*}P < 0.05$, $^{**}P < 0.01$, and $^{***}P < 0.001$. Scram, scrambled.

negatively affect hVSMC cell cycle progression and proliferation. First, BrdU incorporation determined that cell proliferation of FXR1-depleted hVSMC was significantly reduced compared with scrambled control cells (Figure 4A). Next, hVSMC were subject to cell cycle analysis by PI staining and flow cytometry. Figure 4B is a representative experiment showing that in asynchronously growing hVSMC, a significantly greater number of FXR1-depleted cells were in G1, and there were significantly fewer proliferating cells (S and G2/M phase) in FXR1-depleted cells compared with scrambled control cells. A compilation of four asynchronous experiments and five experiments where hVSMC were synchronized by fetal calf depletion are depicted in Figure 4C, and together, demonstrate that

A

ARE	3′ UTR	Total intronic
CDK1	12	68
CDKN3	0	54
BUB1	1	102
MKi67	2	47

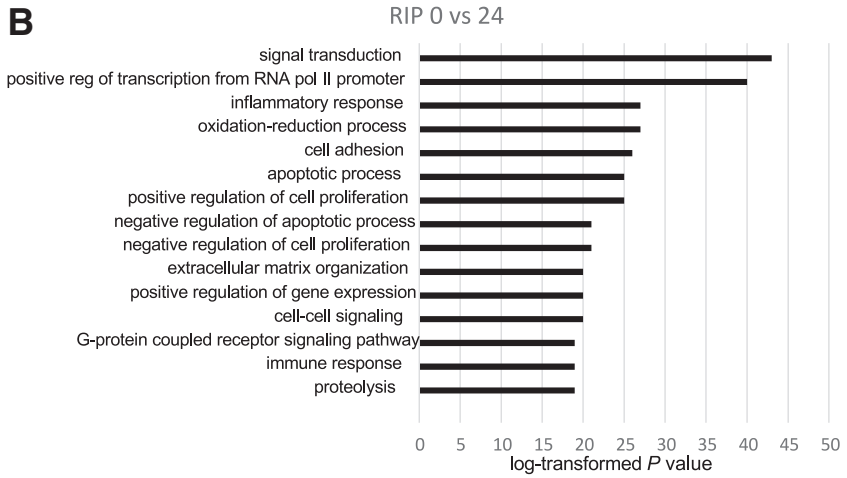

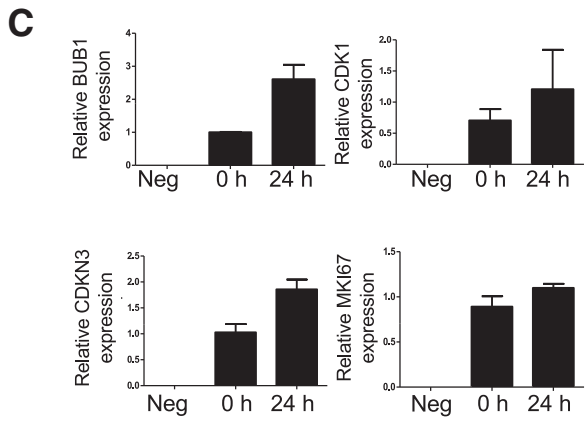

Figure 3 RNA-immunoprecipitation (RIP) sequencing. Human vascular smooth muscle cells (hVSMC) were infected with FLAG-tagged FXR1 adenovirus, serum-starved and stimulated with TNFα for 24 hours. **A:** Table showing number and location of adenine and uridine-rich elements (ARE) in CDK1, CDKN3, BUB1, and MKI67 mRNA. **B:** FXR1 RIPseq. Gene Ontology of RIPseq comparing transcripts immunoprecipitated in unstimulated with TNFα-stimulated hVSMC. **C:** Cell division—associated transcripts detected by RNAseq independently validated by immunoprecipitation with FLAG-tagged FXR1 in unstimulated and stimulated hVSMC. Neg, negative; UTR, untranslated regions.

hVSMC depleted of FXR1 are less proliferative compared with control cells.

Several cellular and molecular approaches were used to test the possibility that impairment of cell cycle progression may predispose the cells to senescence. First, after transfection with FXR1 siRNA or scrambled control, hVSMC were seeded on chamber slides, and after 72 hours, stained for beta-galactosidase activity, a common readout for cellular senescence.[31] Figure 5A shows that FXR1-depleted hVSMC had significantly more beta-galactosidase–positive cells compared with control cells (10.85 ± 1.42 versus 33.17 ± 1.12 positive cells, $P < 0.001$ for scrambled control and FXR1 siRNA, respectively). In a second experiment, FXR1-depleted and control hVSMC were immunostained with phospho-γH2AX, a marker of DNA damage associated with senescence.[32] Nuclear punctate staining was significantly increased in FXR1 hVSMC compared with control cells [12.82 ± 2.58 versus 33/70 ± 6.05 cells/high power field (HPF), $P < 0.001$, for scrambled versus FXR1 siRNA, respectively] (Figure 5B). Expression of a number of cytokines and related genes of the senescence-associated secretory phenotype (SASP) is indicative of senescent cells.[33] hVSMC transfected with FXR1 siRNA or a scrambled control were tested for expression of genes considered to be part of the SASP. Figure 5C indicates that numerous recognized SASP markers, including HMGB1, HMBG2, CXCL11, IL-1α, IL-6, and MCP1, were all significantly increased in FXR1-depleted hVSMC. Increased p53 expression is an obligate event in senescence, and Figure 5D demonstrates that p53 abundance is significantly increased in FXR1-depleted hVSMC, indicative of senescence. Together, these data strongly suggest that depletion of FXR1 results in decreased hVSMC cell proliferation, which may induce a senescent phenotype in these cells.

Genetic Deletion of FXR1 from VSMC Reduces Neointima Formation

To test the hypothesis that FXR1 participates in the development of vascular disease, SMC-specific FXR1 conditional

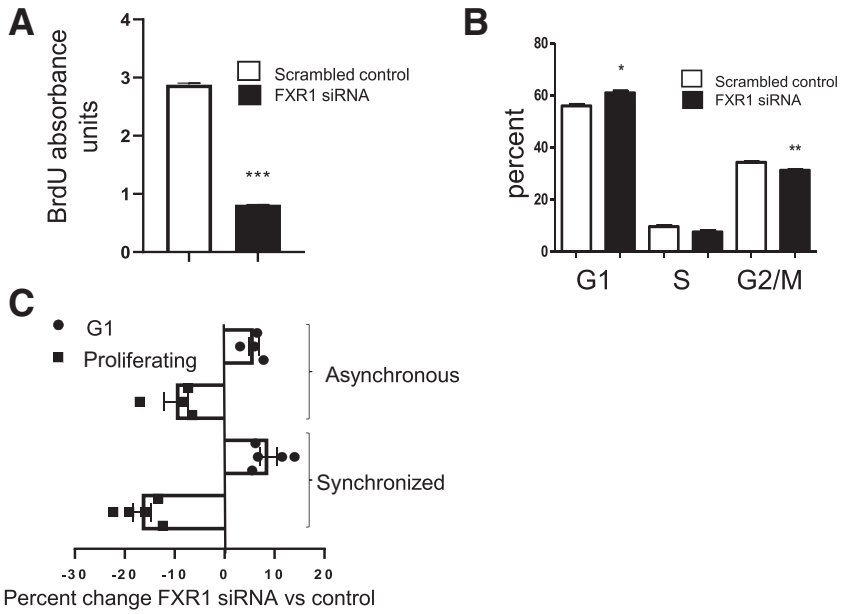

Figure 4 FXR1 knockdown reduces human vascular smooth muscle cells (hVSMC) proliferation. **A:** hVSMC transfected with FXR1 siRNA incorporate significantly less bromodeoxyuridine (BrdU) compared with control siRNA. **B:** Representative cell cycle analysis of asynchronously growing FXR1-depleted and scrambled control hVSMC analyzed by propidium iodide staining and flow cytometry. There are significantly more cells in the G1 phase of the cell cycle and significantly fewer cycling cells overall among cells treated with FXR1 siRNA compared with controls. $P = 0.067$ for S phase. **C:** Compilation of four asynchronously growing and five synchronized FXR1-depleted and scrambled control hVSMC analyzed by propidium iodide staining and flow cytometry, all independent experiments. $*P < 0.05$, $**P < 0.01$, and $***P < 0.001$.

knockout mice were generated. Figure 6A shows that tamoxifen injection reduced FXR1 protein abundance in the aorta, and Figure 6B is quantitative RT-PCR showing tissue-specific and tamoxifen-inducible FXR1 deletion. These mice were subject to carotid artery ligation to induce neointimal hyperplasia, which is primarily a VSMC-driven proliferative disease model.[34–36] Figure 6, C and D, shows that tamoxifen-injected $FXR1^{SMC/SMC}$ mice developed significantly less neointimal hyperplasia compared with control mice. There was no significant difference in intima/media ratios among the control groups. However, $FXR1^{SMC/SMC}$ injected with tamoxifen demonstrated a significantly lower intima/media ratio compared with oil-injected and all other controls (0.93 ± 0.11 versus 0.45 ± 0.04, $P < 0.001$ for oil and tamoxifen injected, respectively). Together, these data indicate that FXR1 participates in development of vascular restenosis, as absence of FXR1 reduces ligation-induced neointimal hyperplasia.

It was important to provide mechanistic insight to support the effects of FXR1 depletion on reduction of neointimal hyperplasia. Initially, the study attempted to isolate and culture VSMC from tamoxifen-injected $FXR1^{SMC/SMC}$ mice, normally a routine procedure, but the mVSMC could not be passaged past their initial isolation to generate cell numbers that were sufficient to perform appropriate subsequent studies. Considering that senescence was induced in hVSMC depleted of FXR1 by siRNA, together with the inability to propagate aortic VSMC from tamoxifen-injected $FXR1^{SMC/SMC}$ mice, experiments were performed to test the possibility that VSMC isolated from these mice were senescent. One experiment that required a very limited number of VSMC was to quantitate beta-galactosidase activity in mVSMC isolated from $FXR1^{SMC/SMC}$ mice injected with tamoxifen and oil-injected control mice. Figure 7A shows that VSMC isolated from tamoxifen-injected mice had significantly more beta-galactosidase activity compared with controls (1.94 ± 1.23 cells/HPF versus 14.05 ± 2.29 cells/HPF, $P < 0.01$ for $FXR1^{flox/flox}$ and $FXR1^{SMC/SMC}$ + tamoxifen, respectively). In a second approach to garner additional cells to test this hypothesis, beta-galactosidase activity was compared in VSMC isolated from $FXR1^{SMC/SMC}$ mice transduced with AdCre, AdGFP, or AdFXR1 viruses. Figure 7B shows that AdCre was effective at reducing FXR1 protein and mRNA expression. Figure 7A also shows that $FXR1^{SMC/SMC}$ VSMC transduced with AdCre had significantly more beta-galactosidase activity compared with AdGFP and AdFXR1 control cells (32.41 ± 4.25 cells/HPF versus 4.64 ± 2.22 cells/HPF, $P < 0.001$ for AdCre and AdGFP, respectively). AdCre-transduced $FXR1^{SMC/SMC}$ VSMC were then used to determine whether decreased abundance of the cell division genes identified in RNA-seq of hVSMC were also decreased in AdCre-treated $FXR1^{SMC/SMC}$ mVSMC. Figure 7C shows that expression of CDK1, CDKN3, and MKI67 were significantly decreased in these cells, which is what was observed in hVSMC. It was next determined that expression of senescence-associated genes p16, p21, and p53 were significantly increased in AdCre-transduced mVSMC (Figure 7D), supporting the beta-galactosidase and γH2AX results. Importantly, mRNA stability of these senescence-associated transcripts was not increased with FXR1 deletion, indicating that the increase in mRNA abundance was due to increased senescence, not FXR1-mediated increase in mRNA stability (Figure 7E). Together, the increase in multiple readouts of senescence was consistent with what was observed in hVSMC depleted of FXR1 by siRNA, and when taken together indicates that VSMC depleted of FXR1 assume a senescent phenotype.

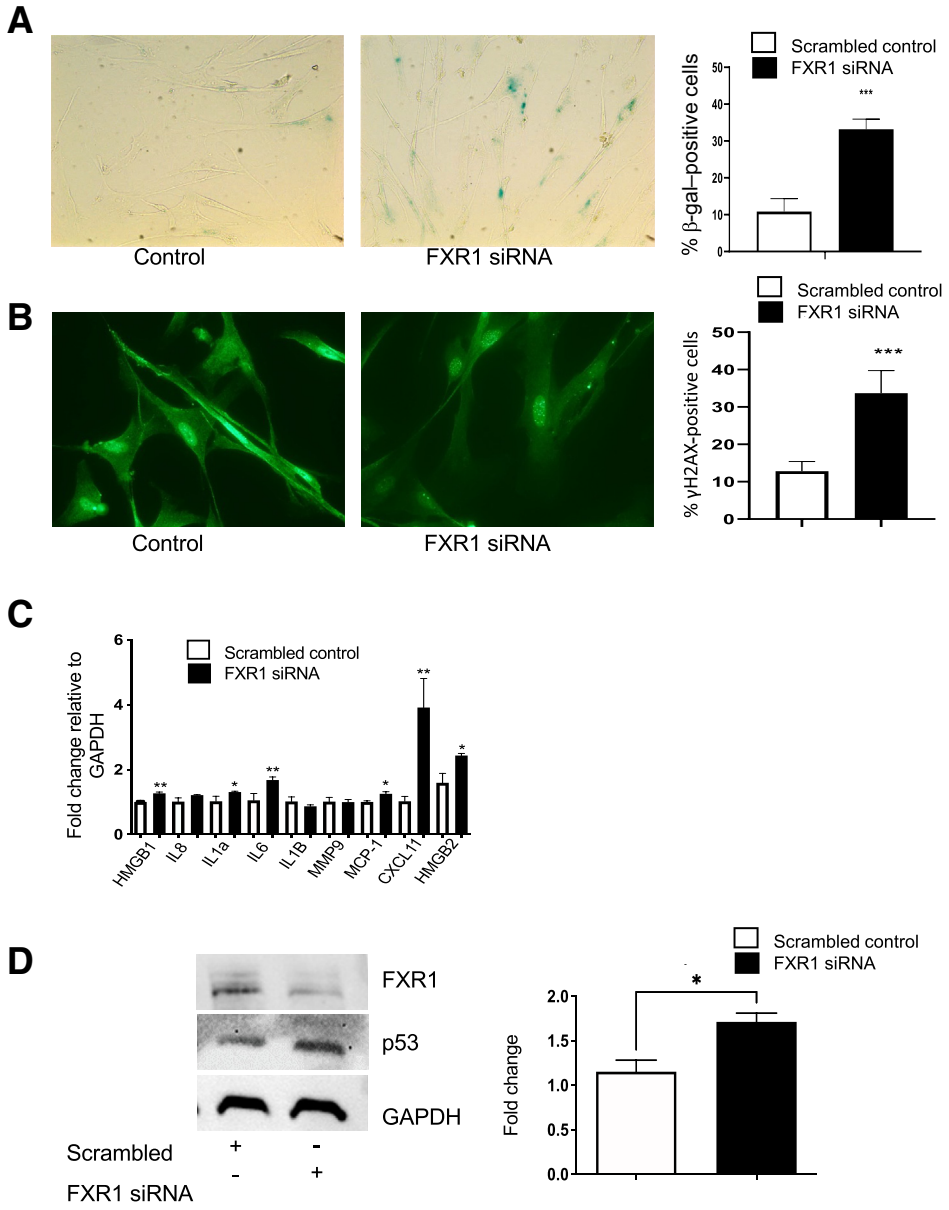

Figure 5 FXR1 knockdown induces senescence. **A:** FXR1-depleted human vascular smooth muscle cells (hVSMC) become senescent. hVSMC transfected with FXR1 or control siRNA were seeded on glass chamber slides and stained for beta-galactosidase. Percent positive cells were quantitated by counting cells per high power field. **B:** FXR1-depleted and scrambled control hVSMC were immunostained with γH2AX. Punctate nuclear staining indicates positivity. Percent positive nuclei were quantitated by counting nuclei per high power field. **C:** FXR1-depleted hVSMC display significantly increased senescence-associated secretory phenotype—associated gene expression compared with control cells. hVSMC transfected with FXR1 or control siRNA were serum-starved, then RNA was isolated, reverse transcribed, and amplified with primers to the genes shown. **D:** Representative Western blot showing that there is significantly increased expression of p53 following knockdown of FXR1 in hVSMC. $n \geq 3$ experiments (**A** and **B**); $n = 4$ high power fields (**A** and **B**). $^{*}P < 0.05$, $^{**}P < 0.01$, and $^{***}P < 0.001$. Original magnification: 20× (**A**); 40× (**B**).

Deletion of FXR1 Induces VSMC Senescence *in Vivo*

Experiments were then done to test the hypothesis that the neointimal hyperplasia reduction observed in the ligated carotid arteries would be due to induction of senescence. RNA was isolated from ligated and unligated carotid arteries from tamoxifen- and oil-injected $FXR1^{SMC/SMC}$ mice and expression of cell division-related genes quantitated by quantitative RT-PCR. Figure 8A shows that similar to cultured human and murine VSMC depleted of FXR1 *in vitro*, abundance of BUB1 and CDK1 mRNA was significantly reduced in ligated carotid arteries from tamoxifen-injected mice compared with control mice. Expression of senescence-associated genes was also increased in these arteries. Figure 8B shows that p21, p53, and HMGB1 mRNA expression is significantly increased in carotid arteries from tamoxifen-injected mice compared with control mice. Importantly, p53 protein expression, an obligate event in p21 expression and cellular senescence, is significantly increased in FXR1-depleted carotid arteries

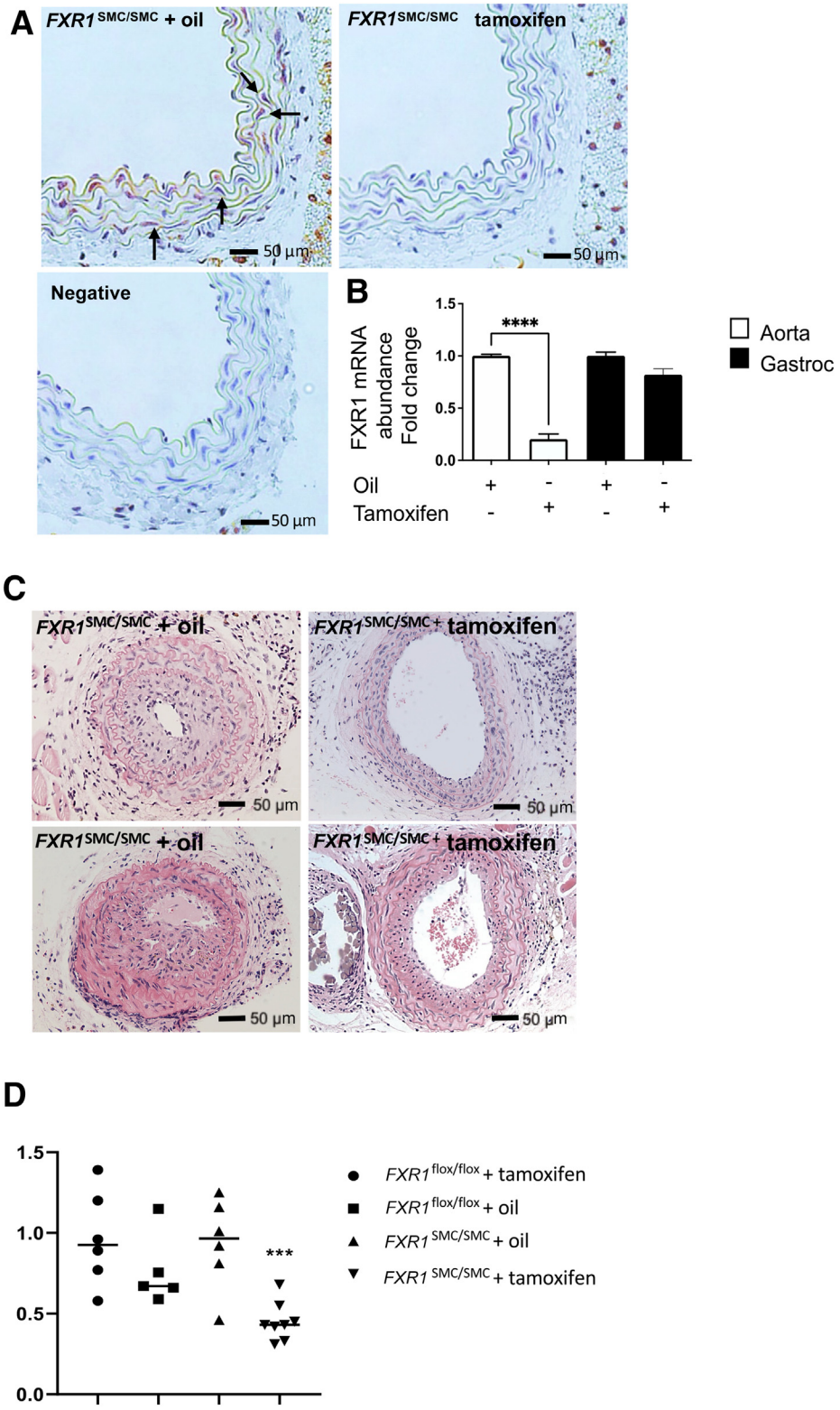

Figure 6 *FXR1*$^{SMC/SMC}$ knockout mice have reduced neointimal formation in response to carotid artery ligation. **A:** Vascular smooth muscle cells (VSMC)-specific FXR1 knockout mice express reduced FXR1 in smooth muscle cells. Immunohistochemical staining of mouse aorta with FXR1-specific antibody demonstrates absence of immunoreactivity in media of aorta in tamoxifen-injected mice. **B:** Quantitative RT-PCR from RNA isolated from various muscle tissue shows reduced expression of FXR1 protein in aorta in tamoxifen-injected mice, but not in oil-injected mice, and no reduction in skeletal muscle. **C:** Representative cross sections of carotid arteries from oil- and tamoxifen-injected mice 28 days after ligation stained with hematoxylin and eosin showing decreased neointimal formation. **D:** Quantitation of neointimal formation from oil- and tamoxifen-injected *FXR1*$^{SMC/SMC}$ mice, as well as control mice injected with oil and tamoxifen. *FXR1*$^{SMC/SMC}$ mice injected with tamoxifen have significantly less neointimal formation compared with all other control mice. ***$P < 0.001$, ****$P < 0.0001$ compared with oil injected *FXR1*$^{SMC/SMC}$ mice. Scale bars = 50 μm. Gastroc, gastrocnemius; I/M, intima/media.

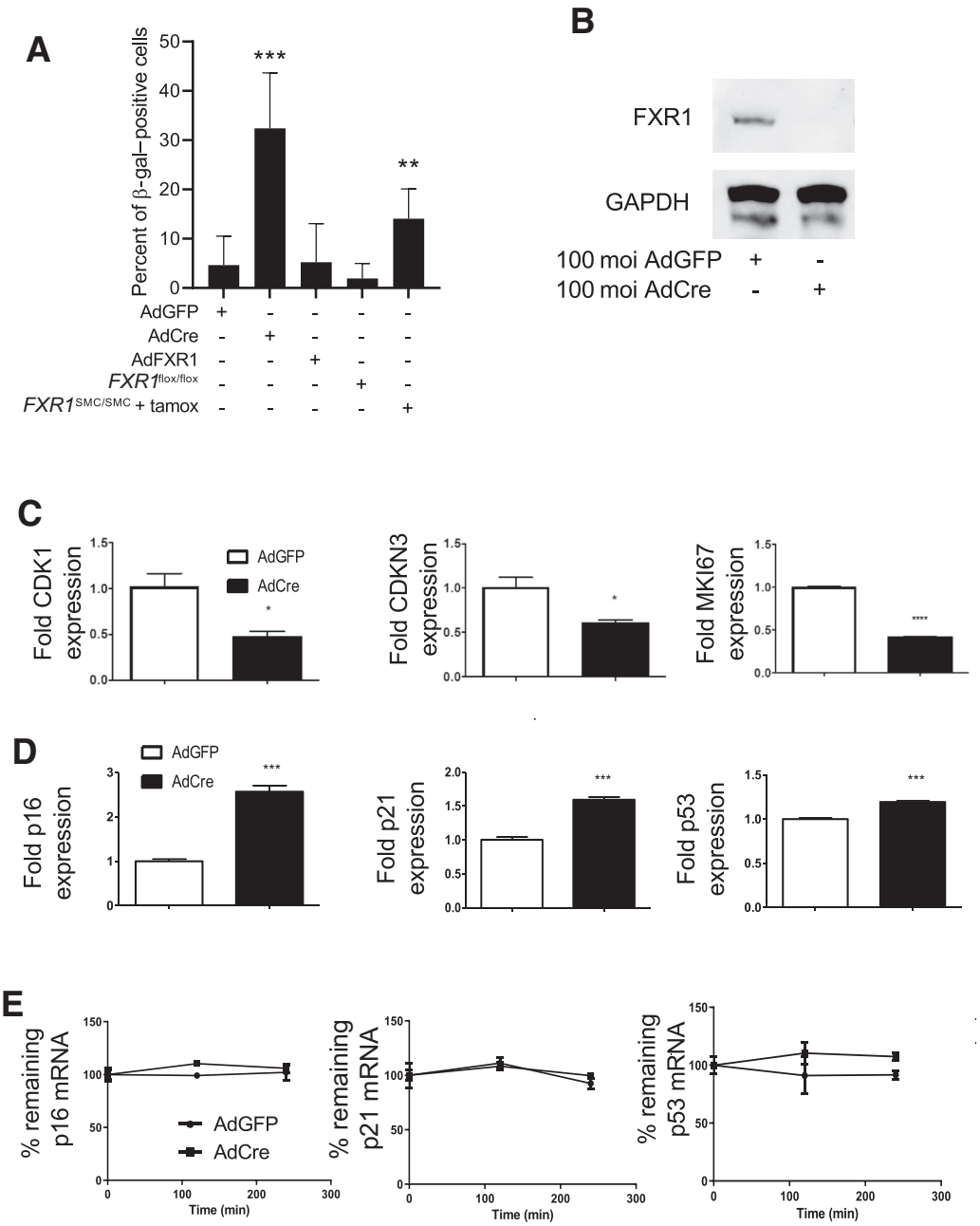

Figure 7 Mouse vascular smooth muscle cells (mVSMC) depleted of FXR1 are senescent and have reduced expression of cell cycle—associated genes. **A:** mVSMC isolated from oil- or tamoxifen-injected (tamox) *FXR1*$^{SMC/SMC}$ mice, and mVSMC isolated from FXR1$^{fl/fl}$ mice transduced with AdGFP or AdCre were seeded on glass chamber slides, and stained for beta-galactosidase activity. **B:** Protein extracts from mVSMC isolated from *FXR1*$^{SMC/SMC}$ mice transduced with AdGFP or AdCre show reduction of FXR1 expression. **C:** Abundance of cell division—associated genes identified by RNAseq in FXR1 depleted hVSMC are also significantly decreased in AdCre-transduced *FXR1*$^{SMC/SMC}$ mVSMC detected by quantitative RT-PCR. **D:** Abundance of senescence-associated genes are significantly increased in AdCre-transduced *FXR1*$^{SMC/SMC}$ mVSMC detected by quantitative RT-PCR. **E:** senescence-associated genes do not have reduced mRNA stability in FXR1-depleted mVSMC. *$P < 0.05$, **$P < 0.01$, ***$P < 0.001$, and ****$P < 0.0001$. moi, multiplicity of infection.

(Figure 8C), further validating a senescent state of aortic VSMC. Together, this suggests that at least one mechanism whereby *FXR1*$^{SMC/SMC}$ mice have reduced neointimal formation is due to reduced expression of cell cycle and proliferative transcripts as well as increased senescence-associated transcripts in arterial VSMC.

Discussion

The present study tested the overarching hypothesis that FXR1, a muscle-enhanced protein, participates in the VSMC response to vascular injury. Initially, it was determined that FXR1 mRNA and protein abundance were

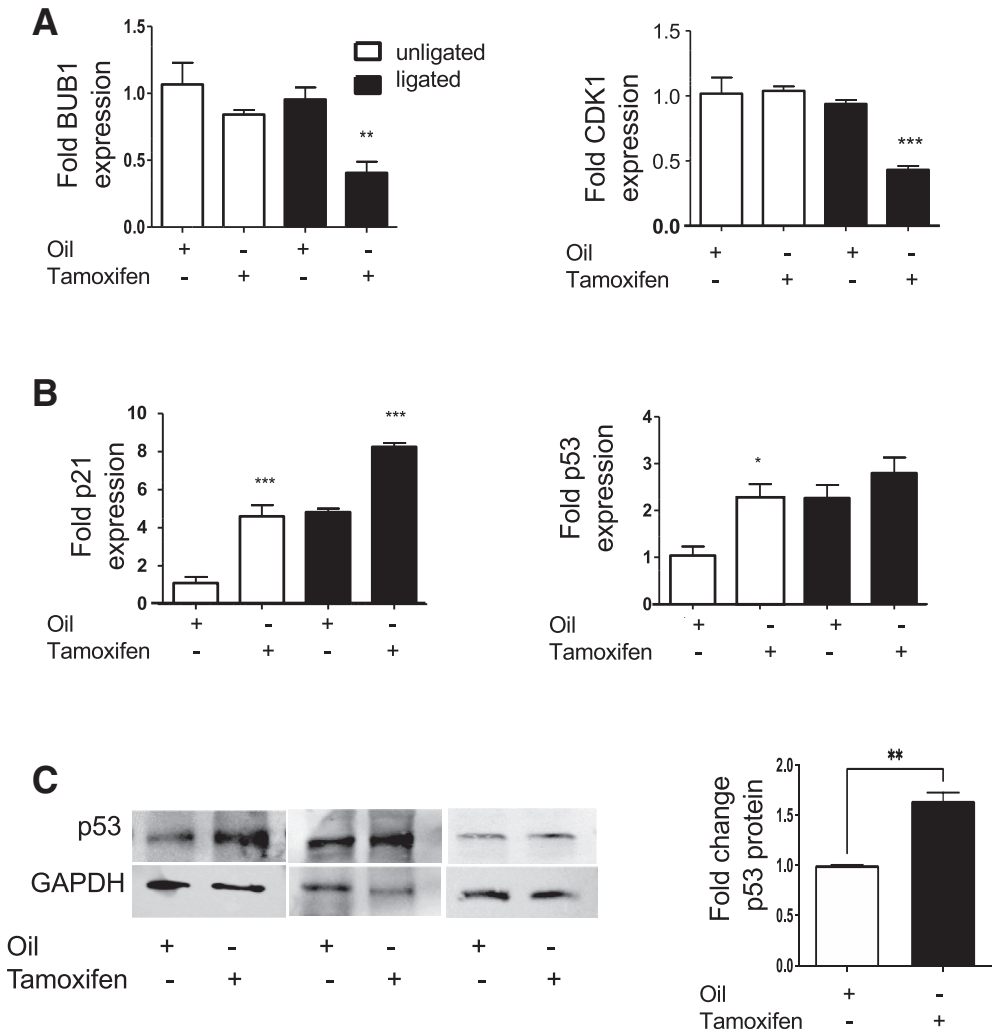

Figure 8 Decreased cell division–associated and increased senescence gene expression in ligated carotid arteries from *FXR1*$^{SMC/SMC}$ mice. **A:** Carotid arteries from tamoxifen- and oil-injected mice were ligated as described in Figure 6. Twenty-eight days later, total RNA was extracted, and quantitative RT-PCR of select cell division–associated genes identified by RNAseq in FXR1-depleted hVSMC were identified as significantly decreased. **B:** Abundance of senescence-associated genes is significantly increased in tamoxifen-injected mice compared with oil-injected control mice detected by quantitative RT-PCR. **C:** p53 protein is increased in carotid arteries in tamoxifen-injected mice detected by Western blot, indicating senescence. Western blot is shown, and densitometry is from the Western blots. $n = 3$ pairs of mice (**C**).*$P < 0.05$, **$P < 0.01$, and ***$P < 0.001$.

increased in primary hVSMC challenged with TNFα, suggesting that FXR1 might participate in regulation of inflammation-responsive transcripts. RNA-sequencing in hVSMC depleted of FXR1 indicated a particularly large number of transcripts that were up-regulated, consistent with our understanding of FXR1 as an mRNA destability RBP. However, intriguingly, a smaller number of transcripts appeared to be decreased in the absence of FXR1, which was unexpected. Importantly, in TNFα-stimulated VSMC, the overwhelming majority (29 of 32) of these transcripts were associated with regulation of cell division, including cell cycle progression, mitotic checkpoints, and chromosome assembly during mitosis. BUB1 is a serine/threonine protein kinase that phosphorylates mitotic checkpoint complex proteins ensuring correct chromosome alignment,[37] and it is required for ensuring proper chromosome segregation.[38] CDK1 is a serine/threonine protein kinase and a component of the M-phase promoting complex, which is essential for G1/S and G2/M phase transitions.[39,40] CDK1 also modulates association and phosphorylation of multiple cyclins that regulate S-phase and mitotic cyclins.[40] CDKN3 is an inhibitor of cyclin-dependent kinases and is overexpressed in many different cancers.[41,42] MKI67 is a marker for cellular proliferation and is necessary component for cell division because it associates with and is required to maintain mitotic chromosome separation during cell division.[43,44] Knockdown of FXR1 in VSMC in the presence of the transcription inhibitor actinomycin D resulted in significantly decreased mRNA stability of many of these transcripts, which suggested that their decreased mRNA abundance was likely due to reduced mRNA stability, counter to current thinking

that FXR1 is an mRNA destability factor. FXR1 is noted for its ability to destabilize mRNA, most notably TNFα mRNA,[12,14,45] but there are few reports of FXR1 acting to stabilize mRNA. One report in a prostate cancer cell line suggests that FXR1 participated in, but was not solely responsibility for, stabilization of desmoplakin mRNA in a prostate cancer cell line.[46] Overexpression of FXR1 in neonatal rat myocytes increased Cx45 mRNA levels, but neither mRNA stability nor effect of FXR1 knockdown on Cx45 expression was examined.[47]

The decrease in cell division–associated proteins provided impetus to determine whether depletion of FXR1 would decrease TNFα-driven cellular proliferation. Knockdown of FXR1 in primary hVSMC led to decreased proliferation of these cells. Reduction of FXR1 in other cell systems has also been seen to influence cell proliferation. In a recent study, knockdown of FXR1 reduced keloid-derived proliferation, but we concluded this was due to induction of apoptosis in these cells.[48] Differences in apoptotic protein mRNA in either the RNAseq or the RIPseq analysis were not detected in the current study. Another study determined that deletion of FXR1 in neural stem cells results in decreased generation of new neurons, but the mechanisms were not discussed.[49]

Cellular senescence is stable, irreversible cell cycle arrest and is closely associated with a decrease in proliferation.[15] There are no reports in the literature associating FXR1 expression with senescence in primary cells. The present study found that two indices of senescence, increased beta-galactosidase staining and γH2AX-positive nuclei were increased in primary hVSMC depleted of FXR1. This is consistent with one other report linking FXR1 with senescence in a murine cancer cell line,[50] and differs from that work in that the current study utilized primary hVSMC.

Senescent cells exhibit phenotypic changes called the SASP characteristic of a senescent cell, which includes increased secretion of inflammatory cytokines, growth factors, and chemokines that all lead to increased inflammation in the tissue microenvironment.[17,51] Many of these soluble factors contribute to vascular occlusive diseases. With this in mind, the study investigated the expression of transcripts to be associated with the senescent phenotype.[52] Six of nine genes examined were significantly increased in siRNA-treated hVSMC, indicating that depletion of FXR1 from primary hVSMC initiates SASP expression. Although SASP expression validates that hVSMC depleted of FXR1 are senescent, it cannot determine whether these soluble factors are contributing to VSMC senescence *in vivo*.

Proliferation of intimal VSMC is a major cellular event in the development of vascular restenosis and atherosclerosis.[53,54] VSMC senescence and death are hallmarks of advanced atherosclerotic lesions, and recent evidence supports a direct causative role of SMC senescence in atherosclerotic plaque progression to the rupture-prone necrotic stage.[55] FXR1 expression is increased in injured arteries and acted as a destability factor for inflammatory mRNA, but direct causality for FXR1 expression in vascular disease needed to be established.[14] Expression of FXR1 is muscle-enhanced, and FXR1 has been referred to as the muscle-specific FMR1 family member, suggesting a specialized function in muscle tissue.[12,13] Total knockout of FXR1 is postnatally lethal,[49] displaying a striated muscle phenotype, providing rational for the generation of SMC-specific conditional knockout mice. $FXR1^{SMC/SMC}$ mice subject to carotid artery ligation demonstrated significantly reduced neointimal formation compared with controls, suggesting a central role for this RBP in VSMC pathophysiological processes.

To characterize the molecular mechanisms of reduced neointimal formation observed in the $FXR1^{SMC/SMC}$ mice, aortic VSMC from FXR1 knockout mice were initially explanted and cultured. However, although a routine procedure, culturing of these cells past the initial isolation proved difficult, which prevented obtaining numbers sufficient for characterizing and validating the senescence of the primary hVSMC depleted of FXR1. Therefore, an alternative approach of transducing mVSMC cultured from $FXR1^{SMC/SMC}$ mice with AdCre was used, which successfully knocked out FXR1 expression. Interestingly, this approach was utilized by other investigators who were unable to grow freshly isolated neural cells from FXR1 knockout mice.[49] Importantly, these mVSMC phenocopied hVSMC depleted of FXR1 by siRNA and showed increased indices of senescence, including β-gal staining and increased expression of proteins associated with the senescent phenotype. These mVSMC also showed decreased expression of some of the same cell cycle–associated proteins that were destabilized in hVSMC.

We hypothesized that genetic deletion of FXR1 from VSMC results in significantly reduced neointima formation by decreased abundance of cell cycle proteins and induction of cellular senescence. Indeed, carotid arteries from $FXR1^{SMC/SMC}$ mice injected with tamoxifen demonstrated significantly less expression of cell cycle–related genes initially identified in RNAseq from hVSMC. Importantly, expression of p21 and p53, recognized markers of senescence, was significantly increased in $FXR1^{SMC/SMC}$ arteries. Their increased expression is likely because of the senescent phenotype of the aortic VSMC, and not because FXR1 modulates their mRNA stability. This strongly suggests that one likely reason that deletion of FXR1 results in decreased neointima formation is through induction of senescence in medial VSMC in ligated carotid arteries. FXR1 has been reported to regulate p21 mRNA stability, effecting cancer cell line senescence.[56] However, a decrease in p21 mRNA stability was not observed in the current study, which may reflect cell type–dependent differences or distinctions between primary cells and transformed cell lines.

There are limitations in this work that future studies could address. The precise molecular mechanism(s) of how FXR1 regulates mRNA stability of cell division–related transcripts needs to be elucidated. It would also be informative

to determine the percent of senescent VSMC in $FXR1^{SMC/SMC}$ aorta, and the functionality of such aorta in which FXR1 was depleted. Although it is likely that depletion of FXR1 results in decreased abundance of cell division proteins and decreased hVSMC cell proliferation resulting in a senescent phenotype in these cells, we cannot determine a direct effect of SASP factors in modulation and maintenance of this senescent phenotype.

In summary, this work shows that FXR1, a muscle-enhanced RBP recognized as a destabilizing RBP, stabilizes a select group of mRNA transcripts associated with cell division. Depletion of FXR1 from VSMC reduces their proliferation and induces senescence, which is likely a mechanism for reduced neointimal formation observed in ligated carotid arteries from $FXR1^{SMC/SMC}$ mice. These data suggest that FXR1 expression and/or RNA binding activity would make an attractive target for modalities to combat vascular proliferative diseases.

References

1. Allahverdian S, Chehroudi AC, McManus BM, Abraham T, Francis GA: Contribution of intimal smooth muscle cells to cholesterol accumulation and macrophage-like cells in human atherosclerosis. Circulation 2014, 129:1551−1559
2. Raines EW, Ferri N: Thematic review series: the immune system and atherogenesis. Cytokines affecting endothelial and smooth muscle cells in vascular disease. J Lipid Res 2005, 46:1081−1092
3. Ross R: Atherosclerosis–an inflammatory disease. N Engl J Med 1999, 340:115−126
4. Eberhardt W, Doller A, Akool E-S, Pfeilschifter J:: Modulation of mRNA stability as a novel therapeutic approach. Pharmacol Ther 2007, 114:56−73
5. Schoenberg D, Maquat L: Regulation of cytoplasmic mRNA decay. Nat Rev Genet 2012, 13:246−259
6. Hao S, Baltimore D: The stability of mRNA influences the temporal order of the induction of genes encoding inflammatory molecules. Nat Immunol 2009, 10:281−288
7. Anderson P: Post-transcriptional control of cytokine production. Nat Immunol 2008, 9:353−359
8. Anderson P: Intrinsic mRNA stability helps compose the inflammatory symphony. Nat Immunol 2009, 10:233−234
9. Barreau C, Paillard L, Osborne HB: AU-rich elements and associated factors: are there unifying principles? Nucleic Acids Res 2005, 33: 7138−7150
10. Bardoni B, Schenck A, Mandel JL: The Fragile X mental retardation protein. Brain Res Bull 2001, 56:375−382
11. Siomi MC, Siomi H, Sauer WH, Srinivasan S, Nussbaum RL, Dreyfuss G: FXR1, an autosomal homolog of the fragile X mental retardation gene. EMBO J 1995, 14:2401−2408
12. Garnon J, Lachance C, Di Marco S, Hel Z, Marion D, Ruiz MC, Newkirk MM, Khandjian EW, Radzioch D: Fragile X-related protein FXR1P regulates proinflammatory cytokine tumor necrosis factor expression at the post-transcriptional level. J Biol Chem 2005, 280: 5750−5763
13. Mientjes EJ, Willemsen R, Kirkpatrick LL, Nieuwenhuizen IM, Hoogeveen-Westerveld M, Verweij M, Reis S, Bardoni B, Hoogeveen AT, Oostra BA, Nelson DL: Fxr1 knockout mice show a striated muscle phenotype: implications for Fxr1p function in vivo. Hum Mol Genet 2004, 13:1291−1302
14. Herman AB, Vrakas CN, Ray M, Kelemen SE, Sweredoski MJ, Moradian A, Haines DS, Autieri MV: FXR1 is an IL-19-responsive RNA-binding protein that destabilizes pro-inflammatory transcripts in vascular smooth muscle cells. Cell Rep 2018, 24:1176−1189
15. Wirth A, Benyó Z, Lukasova M, Leutgeb B, Wettschureck N, Gorbey S, Orsy P, Horváth B, Maser-Gluth C, Greiner E, Lemmer B, Schütz G, Gutkind JS, Offermanns S: G12-G13-LARG-mediated signaling in vascular smooth muscle is required for salt-induced hypertension. Nat Med 2008, 14:64−68
16. Hayashi S, McMahon AP: Efficient recombination in diverse tissues by a tamoxifen-inducible form of Cre: a tool for temporally regulated gene activation/inactivation in the mouse. Dev Biol 2002, 244: 305−318
17. Kim H, Kim M, Im S-K, Fang S: Mouse Cre-LoxP system: general principles to determine tissue-specific roles of target genes. Lab Anim Res 2018, 34:147−159
18. Ellison S, Gabunia K, Richards JM, Kelemen SE, England RN, Rudic D, Azuma Y-T, Munroy MA, Eguchi S, Autieri MV: IL-19 reduces ligation-mediated neointimal hyperplasia by reducing vascular smooth muscle cell activation. Am J Pathol 2014, 184: 2134−2143
19. Gabunia K, Herman AB, Ray M, Kelemen SE, England RN, DeLa Cadena R, Foster WJ, Elliott KJ, Eguchi S, Autieri MV: Induction of MiR133a expression by IL-19 targets LDLRAP1 and reduces oxLDL uptake in VSMC. J Mol Cell Cardiol 2017, 105:38−48
20. Tian Y, Sommerville LJ, Cuneo A, Kelemen SE, Autieri MV: Expression and suppressive effects of interleukin-19 on vascular smooth muscle cell pathophysiology and development of intimal hyperplasia. Am J Pathol 2008, 173:901−909
21. Ray M, Gabunia K, Vrakas CN, Herman AB, Kako F, Kelemen SE, Grisanti LA, Autieri MV: Genetic deletion of IL-19 (interleukin-19) exacerbates atherogenesis in Il19-/-×Ldlr-/- double knockout mice by dysregulation of mRNA stability protein HuR (human antigen R). Arterioscler Thromb Vasc Biol 2018, 38:1297−1308
22. Autieri MV, Carbone CM: Overexpression of allograft inflammatory factor-1 promotes proliferation of vascular smooth muscle cells by cell cycle deregulation. Arterioscler Thromb Vasc Biol 2001, 21: 1421−1426
23. Gabunia K, Jain S, England RN, Autieri MV: Anti-inflammatory cytokine interleukin-19 inhibits smooth muscle cell migration and activation of cytoskeletal regulators of VSMC motility. AJP Cell Physiol 2011, 300:C896−C906
24. Ellison S, Gabunia K, Kelemen SE, England RN, Scalia R, Richards JM, Orr AW, Orr W, Traylor JG, Rogers T, Cornwell W, Berglund LM, Goncalves I, Gomez MF, Autieri MV: Attenuation of experimental atherosclerosis by interleukin-19. Arterioscler Thromb Vasc Biol 2013, 33:2316−2324
25. Sommerville LJ, Xing C, Kelemen SE, Eguchi S, Autieri MV: Inhibition of allograft inflammatory factor-1 expression reduces development of neointimal hyperplasia and p38 kinase activity. Cardiovasc Res 2009, 81:206−215
26. Cuneo AA, Herrick D, Autieri MV: Il-19 reduces VSMC activation by regulation of mRNA regulatory factor HuR and reduction of mRNA stability. J Mol Cell Cardiol 2010, 49:647−654
27. Gillis P, Malter JS: The adenosine-uridine binding factor recognizes the AU-rich elements of cytokine, lymphokine, and oncogene mRNAs. J Biol Chem 1991, 266:3172−3177
28. Akashi M, Shaw G, Hachiya M, Elstner E, Suzuki G, Koeffler P: Number and location of AUUUA motifs: role in regulating transiently expressed RNAs. Blood 1994, 83:3182−3187
29. Bakheet T, Frevel M, Williams BR, Greer W, Khabar KS: ARED: human AU-rich element-containing mRNA database reveals an unexpectedly diverse functional repertoire of encoded proteins. Nucleic Acids Res 2001, 29:246−254
30. Fallmann J, Sedlyarov V, Tanzer A, Kovarik P, Hofacker IL: ARE-site2: an enhanced database for the comprehensive investigation of AU/GU/U-rich elements. Nucleic Acids Res 2016, 44:D90−D95
31. Dimri GP, Lee X, Basile G, Acosta M, Scott G, Roskelley C, Medrano EE, Linskens M, Rubelj I, Pereira-Smith O: A biomarker

that identifies senescent human cells in culture and in aging skin in vivo. Proc Natl Acad Sci U S A 1995, 92:9363−9367
32. Sedelnikova OA, Horikawa I, Zimonjic DB, Popescu NC, Bonner WM, Barrett JC: Senescing human cells and ageing mice accumulate DNA lesions with unrepairable double-strand breaks. Nat Cell Biol 2004, 6:168−170
33. Liao Z, Yeo HL, Wong SW, Zhao Y: Cellular senescence: mechanisms and therapeutic potential. Biomedicines 2021, 9:1769
34. Xu Q: Mouse models of arteriosclerosis: from arterial injuries to vascular grafts. Am J Pathol 2004, 165:1−10
35. Harmon KJ, Couper LL, Lindner V: Strain-dependent vascular remodeling phenotypes in inbred mice. Am J Pathol 2000, 156: 1741−1748
36. Carmeliet P, Moons L, Collen D: Mouse models of angiogenesis, arterial stenosis, atherosclerosis and hemostasis. Cardiovasc Res 1998, 39:8−33
37. Klebig C, Korinth D, Meraldi P: Bub1 regulates chromosome segregation in a kinetochore-independent manner. J Cell Biol 2009, 185:841−858
38. Kiyomitsu T, Obuse C, Yanagida M: Human Blinkin/AF15q14 is required for chromosome alignment and the mitotic checkpoint through direct interaction with Bub1 and BubR1. Dev Cell 2007, 13: 663−676
39. Timofeev O, Cizmecioglu O, Settele F, Kempf T, Hoffmann I: Cdc25 phosphatases are required for timely assembly of CDK1-cyclin B at the G2/M transition. J Biol Chem 2010, 285:16978−16990
40. Zhang X, Chen Q, Feng J, Hou J, Yang F, Liu J, Jiang Q, Zhang C: Sequential phosphorylation of Nedd1 by Cdk1 and Plk1 is required for targeting of the gammaTuRC to the centrosome. J Cell Sci 2009, 122:2240−2251
41. Gyuris J, Golemis E, Chertkov H, Brent R: Cdi1, a human G1 and S phase protein phosphatase that associates with Cdk2. Cell 1993, 75: 791−803
42. Chinami M, Yano Y, Yang X, Salahuddin S, Moriyama K, Shiroishi M, Turner H, Shirakawa T, Adra CN: Binding of HTm4 to cyclin-dependent kinase (Cdk)-associated phosphatase (KAP).Cdk2.cyclin A complex enhances the phosphatase activity of KAP, dissociates cyclin A, and facilitates KAP dephosphorylation of Cdk2. J Biol Chem 2005, 280:17235−17242
43. Cuylen S, Blaukopf C, Politi AZ, Müller-Reichert T, Neumann B, Poser I, Ellenberg J, Hyman AA, Gerlich DW: Ki-67 acts as a biological surfactant to disperse mitotic chromosomes. Nature 2016, 535: 308−312
44. Booth DG, Takagi M, Sanchez-Pulido L, Petfalski E, Vargiu G, Samejima K, Imamoto N, Ponting CP, Tollervey D, Earnshaw WC, Vagnarelli P: Ki-67 is a PP1-interacting protein that organises the mitotic chromosome periphery. Elife 2014, 3:e01641
45. Khera TK, Dick AD, Nicholson LB: Fragile X-related protein FXR1 controls post-transcriptional suppression of lipopolysaccharide-induced tumour necrosis factor-alpha production by transforming growth factor-beta1. FEBS J 2010, 277:2754−2765
46. Cao H, Gao R, Yu C, Chen L, Feng Y: The RNA-binding protein FXR1 modulates prostate cancer progression by regulating FBXO4. Funct Integr Genomics 2019, 19:487−496
47. Chu M, Novak SM, Cover C, Wang AA, Chinyere IR, Juneman EB, Zarnescu DC, Wong PK, Gregorio CC: Increased cardiac arrhythmogenesis associated with gap junction remodeling with upregulation of RNA-binding protein FXR1. Circulation 2018, 137:605−618
48. Wang B, Yin H, Zhang H, Wang T: circNRIP1 facilitates keloid progression via FXR1-mediated upregulation of miR-503-3p and miR-503-5p. Int J Mol Med 2021, 47:70
49. Patzlaff NE, Nemec KM, Malone SG, Li Y, Zhao X: Fragile X related protein 1 (FXR1P) regulates proliferation of adult neural stem cells. Hum Mol Genet 2017, 26:1340−1352
50. Raheja R, Gandhi R: FXR1: linking cellular quiescence, immune genes and cancer. Cell Cycle 2016, 15:2695−2696
51. Gardner SE, Humphry M, Bennett MR, Clarke MCH: Senescent vascular smooth muscle cells drive inflammation through an interleukin-1α-dependent senescence-associated secretory phenotype. Arterioscler Thromb Vasc Biol 2015, 35:1963−1974
52. Muñoz-Espín D, Serrano M: Cellular senescence: from physiology to pathology. Nat Rev Mol Cell Biol 2014, 15:482−496
53. Doran AC, Meller N, McNamara CA: Role of smooth muscle cells in the initiation and early progression of atherosclerosis. Arterioscler Thromb Vasc Biol 2008, 28:812−819
54. Libby P, Geng YJ, Sukhova GK, Simon DI, Lee RT: Molecular determinants of atherosclerotic plaque vulnerability. Ann N Y Acad Sci 1997, 811:134−142. discussion 142-145
55. Grootaert MOJ, Moulis M, Roth L, Martinet W, Vindis C, Bennett MR, De Meyer GRY: Vascular smooth muscle cell death, autophagy and senescence in atherosclerosis. Cardiovasc Res 2018, 114:622−634
56. Davidovic L, Durand N, Khalfallah O, Tabet R, Barbry P, Mari B, Sacconi S, Moine H, Bardoni B: A novel role for the RNA-binding protein FXR1P in myoblasts cell-cycle progression by modulating p21/Cdkn1a/Cip1/Waf1 mRNA stability. PLoS Genet 2013, 9: e1003367